

# MESON-EXCHANGE MODEL FOR THE $YN$ INTERACTION\*

J. Haidenbauer, W. Melnitchouk and J. Speth

*Institut für Kernphysik, Forschungszentrum Jülich,  
D-52425 Jülich, Germany*

We report on progress in the development of a microscopic model for the hyperon-nucleon interaction within the meson-exchange framework, which incorporates both one-meson as well as correlated two-meson exchange contributions. The main new feature of the model is the exchange of two correlated pions or kaons, both in the scalar-isoscalar and the vector-isovector channels. In the scalar channel it provides the main part of the intermediate-range interaction between two baryons, thereby eliminating the need for the fictitious sigma meson, which has been an unavoidable element of effective one-boson-exchange descriptions.

## 1. INTRODUCTION

The role of strangeness in low and medium energy nuclear physics is currently of considerable interest, as it has the potential to deepen our understanding of the relevant strong interaction mechanisms in the non-perturbative regime of QCD. For example, the system of a strange baryon (hyperon  $Y$ ) and a nucleon ( $N$ ) is in principle an ideal testing ground for investigating the importance of  $SU(3)_{flavor}$  symmetry in hadronic interactions. Existing meson exchange models of the  $YN$  force usually assume  $SU(3)$  flavor symmetry for the hadronic coupling constants, and in some cases [ 1, 2] even the  $SU(6)$  symmetry of the quark model. The symmetry requirements provide relations between couplings of mesons of a given multiplet to the baryon current, which greatly reduce the number of free model parameters. Specifically, coupling constants at the strange vertices are then connected to nucleon-nucleon-meson coupling constants, which in turn are constrained by the wealth of empirical information on  $NN$  scattering. Essentially all these  $YN$  interaction models can reproduce the existing  $YN$  scattering data, so that at present the assumption of  $SU(3)$  symmetry for the coupling constants cannot be ruled out by experiment.

One should note, however, that the various models differ dramatically in the treatment of the scalar-isoscalar meson sector, which describes the baryon-baryon interaction at intermediate ranges. For example, the Nijmegen group [ 3, 4, 5] views this interaction as being generated by genuine scalar meson exchange. In their model D [ 3] an  $\epsilon(760)$  is exchanged as an  $SU(3)_{flavor}$  singlet. In models F [ 4] and NSC [ 5], a scalar  $SU(3)$  nonet is exchanged — namely, two isospin-0 mesons (besides the  $\epsilon(760)$ , the  $\epsilon'(1250)$  in model F and  $S^*(975)$  in model NSC), an isospin-1 meson  $\delta$  and an isospin-1/2 strange meson  $\kappa$ . The Tübingen model [ 6], on the other hand, which is essentially a constituent quark model supplemented by  $\pi$  and  $\sigma$  exchange at intermediate and short ranges, treats the  $\sigma$  meson as an  $SU(3)$  singlet with a mass of 520 MeV.

In the (full) Bonn  $NN$  potential [ 7] the intermediate range attraction is provided by uncorrelated and correlated  $\pi\pi$  exchange processes (Figs. 1(a)–(b) and Fig. 1(c), respectively), with  $NN$ ,  $N\Delta$  and  $\Delta\Delta$  intermediate states. From earlier studies of the  $\pi\pi$  interaction it is known that  $\pi\pi$  correlations are important mainly in the scalar-isoscalar and vector-isovector channels. In one-boson-exchange (OBE) potentials these are included effectively via exchange of sharp mass  $\sigma$  and  $\rho$  mesons. One disadvantage of such

---

\*Presented at Sendai International Workshop on the Spectroscopy of Hypernuclei, January 1998, Sendai, Japan

a simplified treatment is that this parameterization cannot be transferred into the hyperon sector in a well defined manner. Therefore in the earlier  $YN$  interaction models of the Jülich group [ 1], which start from the Bonn  $NN$  potential, the coupling constants of the fictitious  $\sigma$  meson at the strange vertices ( $\Lambda\Lambda\sigma$ ,  $\Sigma\Sigma\sigma$ ) are free parameters — a rather unsatisfactory feature of the models. This is especially true for the extension to the strangeness  $S = -2$  channels, interest in which initiated with the prediction of the H-dibaryon by Jaffe [ 8]. Unfortunately, so far there is no empirical information about these channels.

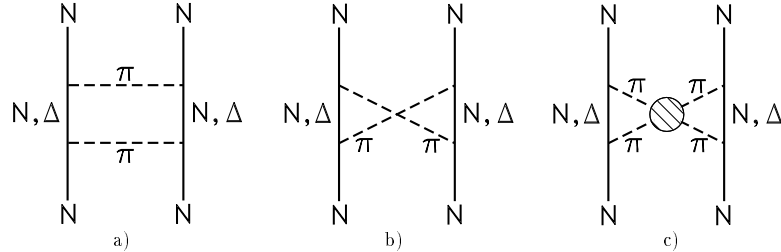


Figure 1. Two-pion exchange in the  $NN$  interaction: (a) uncorrelated iterative and (b) crossed boxes, (c) correlated two-pion exchange.

These problems can be overcome by an explicit evaluation of correlated  $\pi\pi$  exchange in the various baryon-baryon channels. A corresponding calculation was already done for the  $NN$  case (Fig. 1(c)) in Ref. [ 9]. The starting point there was a field theoretic model for both the  $N\bar{N} \rightarrow \pi\pi$  Born amplitudes and the  $\pi\pi$  and  $K\bar{K}$  elastic scattering [ 10]. With the help of unitarity and dispersion relations the amplitude for the correlated  $\pi\pi$  exchange in the  $NN$  interaction was computed, showing characteristic discrepancies with the  $\sigma$  and  $\rho$  exchange in the (full) Bonn potential.

In a recent paper [ 12] the Jülich group presented a microscopic derivation of correlated  $\pi\pi$  exchange in various baryon-baryon ( $BB'$ ) channels with strangeness  $S = 0, -1$  and  $-2$ . The  $K\bar{K}$  channel is treated on an equal footing with the  $\pi\pi$  channel in order to reliably determine the influence of  $K\bar{K}$  correlations in the relevant  $t$ -channels. In this approach one can replace the phenomenological  $\sigma$  and  $\rho$  exchanges in the Bonn  $NN$  [ 7] and Jülich  $YN$  [ 1] models by correlated processes, and eliminate undetermined parameters such as the  $BB'\sigma$  coupling constants [ 13]. The resulting models thus have more predictive power and should allow a more reliable treatment of the  $S = -2$  baryon-baryon channels.

In the next section we describe the basic ingredients used to derive correlated  $\pi\pi$  and  $K\bar{K}$  exchange potentials for the baryon-baryon amplitudes in the  $\sigma$  and  $\rho$  channels. We also give a short outline of the microscopic model for the required  $B\bar{B}' \rightarrow \pi\pi$ ,  $K\bar{K}$  amplitudes. The results for the potentials are presented in Section 3, where we focus on the  $\pi\pi$  correlations in the  $\sigma$  channel. These are compared with the results obtained from the exchange of a sharp mass  $\sigma$  meson in the Bonn  $NN$  [ 7] and Jülich  $YN$  [ 1] potentials. Furthermore, we introduce and discuss results obtained with a parameterization of correlated  $\pi\pi$  and  $K\bar{K}$  exchange potentials by an effective  $\sigma$  exchange for the  $NN$  and  $YN$  channels. Finally, some concluding remarks are made in Section 4.

## 2. MODEL FOR CORRELATED $2\pi$ EXCHANGE

Figure 2 shows a graphic representation of our dynamical model for correlated  $2\pi$  exchange. Here  $B\bar{B}'$  stands for  $N\bar{N}$ ,  $\Lambda\bar{\Lambda}$ ,  $\Lambda\bar{\Sigma}/\Sigma\bar{\Lambda}$  or  $\Sigma\bar{\Sigma}$ . The basic ingredients are the  $B\bar{B}' \rightarrow \pi\pi$ ,  $K\bar{K}$  Born amplitudes and the  $\pi\pi$ - $K\bar{K}$  interaction, which we outline below. Note that a microscopic model of correlated  $\pi\pi$  exchange for the  $NN$  case was already presented in Ref. [ 9]. Interestingly enough, the resulting strength turned out to be considerably larger than that from sharp mass  $\sigma'$  and  $\rho$  exchanges used in the (full) Bonn potential [ 7].

### 2.1. $\pi\pi \rightarrow \pi\pi$ Amplitude

The dynamical model used here is based on the meson exchange framework of Refs. [ 10, 11] involving the  $\pi\pi$  and  $K\bar{K}$  coupled channels. The driving terms for  $\pi\pi \rightarrow \pi\pi$  consist of exchange and pole diagrams (Fig. 3, first and last diagram, respectively) with  $\epsilon \equiv f_0(1440)$ ,  $\rho \equiv \rho(770)$  and  $f_2 \equiv f_2(1274)$  intermediate states. The coupling  $\pi\pi \rightarrow K\bar{K}$  is provided by  $K^*(892)$  exchange, illustrated in the second diagram in Fig. 3.

The bare parameters (masses, coupling constants) in the pole diagrams are dressed by unitarizing the interaction terms in a relativistic Schrödinger equation. The  $K\bar{K} \rightarrow K\bar{K}$  interaction (Fig. 3, third diagram) is strongly isospin dependent: in the scalar-isoscalar channel all contributions ( $\rho$ ,  $\omega$ ,  $\phi$ ) add up and provide a sizable attraction, which leads to a  $K\bar{K}$  bound state at  $f_0(975)$  (see Fig. 4 for the resulting phase shifts) — the genuine scalar resonance  $f_0(1440)$  sits at a higher energy, at about 1.4 GeV. On the other hand, in the vector-isovector channel there is strong cancellation between  $\rho$  and  $\omega$ ,  $\phi$  exchange, since the former changes sign. Consequently, the influence of the  $K\bar{K}$  channel here is negligible. The corresponding phase shift is dominated by the  $\rho$ -pole diagram, as illustrated in Fig. 4.

### 2.2. $B\bar{B} \rightarrow 2\pi$ Helicity Amplitudes

Based on the  $\pi\pi \rightarrow \pi\pi$  amplitude (which has a well defined off-shell behavior) the evaluation of diagrams such as in Fig. 1(c) for any  $B\bar{B}'$  system can be done in two steps. Firstly the  $N\bar{N}$  ( $\Lambda\bar{\Lambda}$ ,  $\Sigma\bar{\Sigma}$ , etc.)  $\rightarrow 2\pi$  amplitudes (illustrated in Fig. 2) are determined in the pseudophysical region ( $t \leq 4m_\pi^2$ ). For the transition Born amplitude,  $V$ , both the  $N$  and  $\Delta$  (or  $\Lambda$ ,  $\Sigma$  and  $Y^*$  in case of  $Y\bar{Y}'$ ) exchanges are taken into account. Corresponding coupling constants in the transition interaction are taken from the Bonn  $NN$  [ 7] and the Jülich  $YN$  potential models [ 1]. Note that this cannot be done for the cutoff masses at the vertices since the form factors now act in quite a different kinematic regime, where the baryon is the essential off-shell particle. For the  $NN$  case, the parameters can be fixed independently (to  $\Lambda_{NN\pi} = 1.9$  GeV,  $\Lambda_{N\Delta\pi} = 2.1$  GeV) by using quasi-empirical information obtained by Höhler at el. [ 14] by analytically continuing the  $\pi N$  and  $\pi\pi$

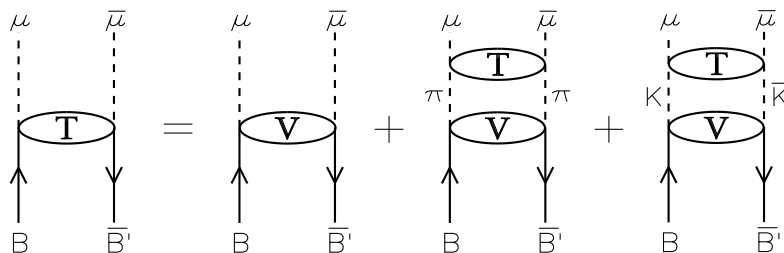


Figure 2. The present dynamical model for the  $B\bar{B} \rightarrow \mu\bar{\mu}$  amplitude ( $\mu\bar{\mu} = \pi\pi, K\bar{K}$ ).

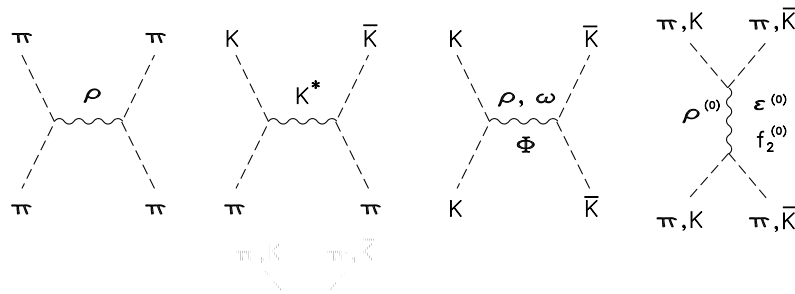


Figure 3. Meson exchange diagrams included in the dynamical model for the  $\pi\pi$ ,  $K\bar{K}$  interaction [ 10].

scattering data. Such information is, however, not available for the  $Y\bar{Y}$  ( $Y = \Lambda, \Sigma$ ) channels, so that here we make the reasonable assumption that  $\Lambda_{\Lambda\Sigma\pi} \simeq \Lambda_{\Sigma\Sigma\pi} \simeq \Lambda_{NN\pi}$  and  $\Lambda_{\Lambda Y^*\pi} \simeq \Lambda_{\Sigma Y^*\pi} \simeq \Lambda_{N\Delta\pi}$ .

### 3. POTENTIAL FROM CORRELATED $\pi\pi$ AND $K\bar{K}$ EXCHANGE

From the  $B\bar{B}' \rightarrow 2\pi$  helicity amplitudes the spectral functions can be calculated (see Ref. [ 12] for details), which are then inserted into dispersion integrals to obtain the (on-shell) baryon-baryon interaction:

$$V_{B'_1, B'_2; B_1, B_2}^{(0^+, 1^-)}(t) \propto \int_{4m_\pi^2}^{\infty} dt' \frac{\rho_{B'_1, B'_2; B_1, B_2}^{(0^+, 1^-)}(t')}{t' - t}, \quad t < 0. \quad (1)$$

We should note that the helicity amplitudes obtained according to Fig. 2 still generate the uncorrelated (first diagram on the r.h.s. of Fig. 2), as well as the correlated pieces (second and third diagrams). Thus, in order to obtain the contribution of the truly correlated  $\pi\pi$  and  $K\bar{K}$  exchange we must eliminate the former from the spectral function. This can be done by calculating the spectral function generated by the Born term and subtracting it from the total spectral function:

$$\rho^{(0^+, 1^-)} \longrightarrow \rho^{(0^+, 1^-)} - \rho_{\text{Born}}^{(0^+, 1^-)}. \quad (2)$$

Note that the spectral functions characterize both the strength and range of the interaction. Clearly, for sharp mass exchanges the spectral function becomes a  $\delta$ -function at the appropriate mass.

It is convenient to present our results in terms of effective coupling strengths, by parameterizing the correlated processes by (sharp mass)  $\sigma$  and  $\rho$  exchanges. The interaction potential resulting from the exchange of a  $\sigma$  meson with mass  $m_\sigma$  between two  $J^P = 1/2^+$  baryons  $A$  and  $B$  has the structure:

$$V_{A, B; A, B}^\sigma(t) = g_{AA\sigma} g_{BB\sigma} \frac{F_\sigma^2(t)}{t - m_\sigma^2}, \quad (3)$$

where a form factor  $F_\sigma(t)$  is applied at each vertex, taking into account the fact that the exchanged  $\sigma$  meson is not on its mass shell. This form factor is parameterized in the conventional monopole form,

$$F_\sigma(t) = \frac{\Lambda_\sigma^2 - m_\sigma^2}{\Lambda_\sigma^2 - t}, \quad (4)$$

with a cutoff mass  $\Lambda_\sigma$  assumed to be the same for both vertices. The correlated potential as given in Eq. (1) can now be parameterized in terms of  $t$ -dependent strength functions  $G_{B'_1, B'_2; B_1, B_2}(t)$ , so that for the  $\sigma$  case:

$$V_{A, A; B, B}^{(0^+)}(t) = G_{A, A; B, B}^\sigma(t) \frac{1}{t - m_\sigma^2}. \quad (5)$$

The effective coupling constants are then defined as:

$$g_{AA\sigma} g_{BB\sigma} \longrightarrow G_{AB \rightarrow AB}^\sigma(t) = \frac{(t - m_\sigma^2)}{\pi F_\sigma^2(t)} \int_{4m_\pi^2}^\infty \frac{\rho_{AB; AB}^{(0^+)}(t')}{t' - t} dt'. \quad (6)$$

Similar relations can be also derived for the correlated exchange in the isovector-vector channel [ 12], which in this case will involve vector as well as tensor coupling pieces.

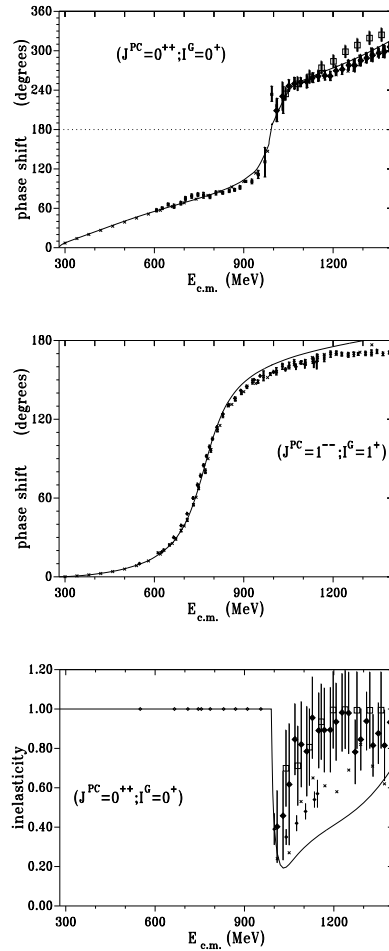


Figure 4.  $\pi\pi$  phase shifts in the  $J^P = 0^+$  ( $\sigma$ ) and  $J^P = 1^-$  ( $\rho$ ) channels and the corresponding inelasticity in the  $\sigma$  channel.

We stress once more that this parameterization does not involve any approximations as long as the full  $t$ -dependence of the effective coupling strengths is taken into account. The parameters of  $\sigma$  and  $\rho$  exchange are chosen to have the same values in all particle channels. The masses  $m_\sigma$  and  $m_\rho$  of the exchanged particles have been set to the values used in the Bonn-Jülich models of the  $NN$  [ 7] and  $YN$  [ 1] interactions,  $m_\sigma = 550$  MeV,  $m_\rho = 770$  MeV. The cutoff masses  $\Lambda_\sigma$  and  $\Lambda_\rho$  have been chosen so that the coupling strengths in the  $S = 0, -1$  baryon-baryon channels vary only weakly with  $t$ . The resulting values ( $\Lambda_\sigma = 2.8$  GeV,  $\Lambda_\rho = 2.5$  GeV) are quite large compared to the values of the phenomenological parameterizations used in Refs. [ 1, 7], and thus represent rather hard form factors.

Note that in the OBE framework the three reactions  $NN \rightarrow NN$ ,  $YN \rightarrow YN$ ,  $YY \rightarrow YY$  are determined by two parameters (coupling constants)  $g_{NN\sigma}$  and  $g_{YY\sigma}$ , whereas the correlated exchanges are characterized by three independent strength functions, so that vertex coupling constants cannot be determined uniquely.

In the physical region the strength of the contributions is to a large extent governed by the value of  $G$  at  $t = 0$ . The values for the various channels are shown in Table 1.

Apart from the values for our full model, Table 1 contains results obtained when uncorrelated contributions involving spin-1/2 baryons only are subtracted from the spectral function of the invariant baryon-baryon amplitudes. These are the proper values to be used for constructing a  $NN$  or  $YN$  model based on simple OBE-exchange diagrams. For the full Bonn  $NN$  model, contributions involving spin-3/2 baryons also need to be subtracted, since the corresponding contributions are already treated explicitly in this model, namely via box diagrams with intermediate  $\Delta$ -states as shown in Fig. 1(a). Obviously processes involving spin-3/2 baryons increase the correlated contribution, in practice by about 30% in all channels.

Comparing the relative strengths of effective  $\sigma$  exchange in the various baryon-baryon channels, one observes that the scalar-isoscalar part of correlated  $\pi\pi$  and  $K\bar{K}$  exchange in the  $NN$  channel is about twice as large as in both  $YN$  channels, and 3 – 4 times larger than in the  $S = -2$  channels.

$G_{AB \rightarrow AB}^\sigma / 4\pi$						
	$NN$	$\Lambda N$	$\Sigma N$	$\Lambda\Lambda$	$\Sigma\Sigma$	$\Xi N$
full model	5.87	2.82	2.58	1.52	1.72	1.19
subtractions for OBE model	7.77	3.81	3.15	2.00	2.31	1.52

Table 1

Effective  $\sigma$  coupling strengths  $G_{AB \rightarrow AB}^\sigma(t = 0)$  for correlated  $\pi\pi$  and  $K\bar{K}$  exchange in the various baryon-baryon channels. (The meaning of the rows is given in the text.)

The average size of the effective coupling strengths is only an approximate measure of the strength of correlated  $\pi\pi$  and  $K\bar{K}$  exchange in the various particle channels. The precise energy dependence of the correlated exchange as well as its relative strength in the different partial waves of the  $s$ -channel reaction is determined by the spectrum of exchanged invariant masses, or spectral functions, leading to a different  $t$ -dependence of the effective coupling strengths. To demonstrate this we show in Fig. 5 the on-shell  $NN$  potentials in spin-singlet states with angular momentum  $L = 0, 2$  and 4, which are generated directly by the scalar-isoscalar part of the correlated  $\pi\pi$  and  $K\bar{K}$  exchange. As expected it is attractive throughout.

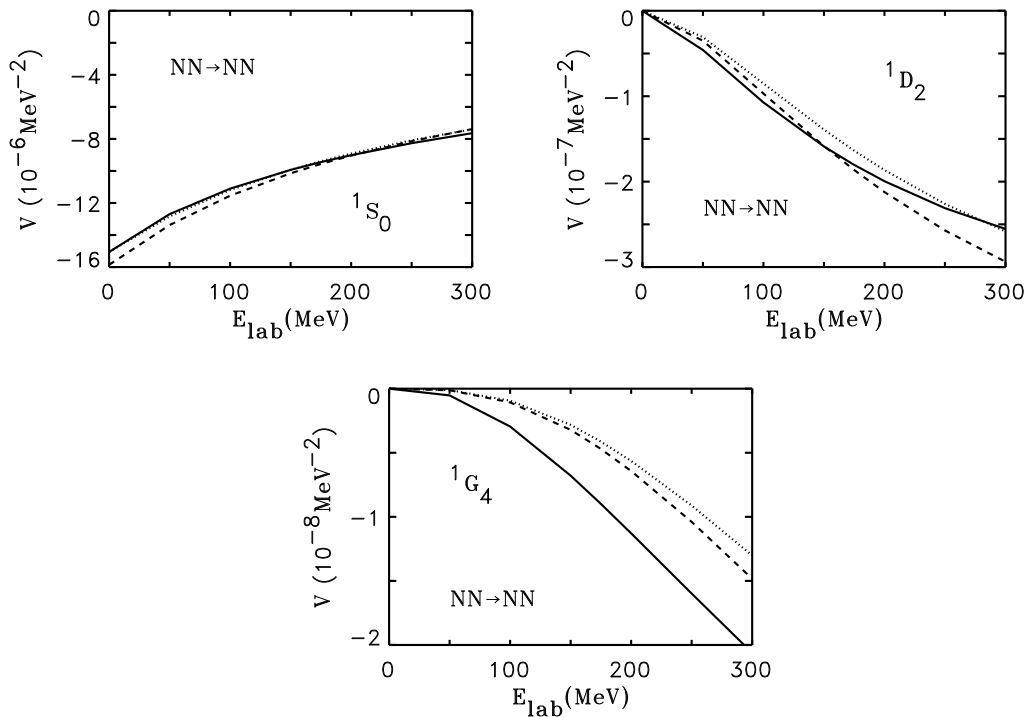


Figure 5. The  $\sigma$ -like part of the  $NN$  on-shell potential in various partial waves. The solid lines are derived from our microscopic model of correlated  $\pi\pi$  and  $K\bar{K}$  exchange. The dotted lines are obtained if the dispersion-theoretic result is parameterized by  $\sigma$  exchange, while the dashed correspond to the  $\sigma$  exchange used in the Bonn OBEPT potential [ 7].

Figure 5 shows that the results evaluated from the microscopic correlated  $2\pi$  exchange model (solid curves) are comparable to those of the  $\sigma$  exchange in the Bonn OBEPT potential (dashed curves) in partial waves with  $J \leq 2$ . However, the correlated  $2\pi$  exchange is significantly stronger in high partial waves because the  $\sigma$  exchange, which corresponds to a spectral function proportional to  $\delta(t' - m_\sigma^2)$ , does not contain the long-range part of the correlated processes. Indeed, parameterizing the results derived from the microscopic model by  $\sigma$  exchange as before, but using the effective coupling strength  $G_{NN \rightarrow NN}^\sigma$  at  $t = 0$  (dotted curves), we obtain rough agreement with the exact result in the  $^1S_0$  partial wave, but underestimate the magnitude considerably in the high partial waves. Obviously the replacement of correlated  $\pi\pi$  and  $K\bar{K}$  exchanges by an exchange of a sharp mass  $\sigma$  meson with a  $t$ -independent coupling cannot provide a simultaneous description of both low and high partial waves.

Note that the above curves are based on the spectral function with subtraction for OBE models. Corresponding results for the full model were presented in Fig. 22 of Ref. [ 12], and differ quantitatively from the ones shown here. In particular, the contribution of the correlated  $\pi\pi$  and  $K\bar{K}$  exchanges in the scalar-isoscalar channel is stronger than the  $\sigma'$  exchange of the full Bonn potential in *all* partial waves — in agreement with earlier results reported in Ref.[ 9].

In Fig. 6 we show the corresponding on-shell matrix elements for the  $\Lambda N$  channel. Also here we see that the results generated by the scalar-isoscalar part of correlated  $\pi\pi$  and  $K\bar{K}$  exchange are comparable to the ones of the  $\sigma$  exchange used in the Jülich  $YN$  model A. In fact, correlated  $\pi\pi$  exchange is slightly stronger in the  $^1S_0$  partial wave, but weaker in the  $^1D_2$  partial wave. Once again we see that the parameterization by an effective  $\sigma$

exchange works well for the lower partial waves ( $J \leq 2$ ), but fails for the higher partial waves.

Finally, Fig. 7 shows the corresponding results for the on-shell  $\Sigma N$  potentials. Here one can see that the  $\sigma$  exchange used in the Jülich  $YN$  model A is clearly much stronger than the results one obtains from the correlated  $\pi\pi$  and  $K\bar{K}$  exchange. These differences will have an impact on the properties of the new hyperon-nucleon interaction model currently being developed [13]. Specifically, the weaker interaction in the scalar-isoscalar channel resulting from our microscopic model of correlated  $\pi\pi$  exchange provides much less attraction in the  $N\Sigma$   $S$ -waves and, in turn, should also reduce the coupling between the  $N\Lambda$  and  $N\Sigma$  channels. The strong coupling between these two systems in the original Jülich  $YN$  model is possibly one of the reasons why it does not lead to a bound state for the hypertriton [15].

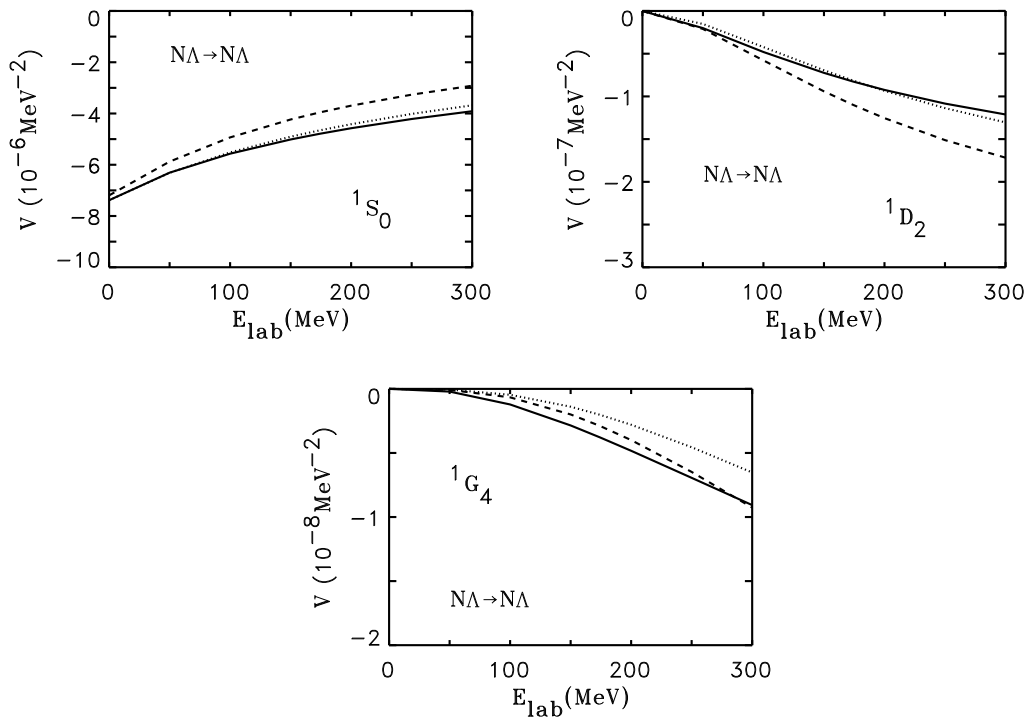


Figure 6. The  $\sigma$ -like part of the  $\Lambda N$  on-shell potential in various partial waves. The curves are as in Fig. 5, except for the dashed lines which correspond to the  $\sigma$  exchange used in the Jülich  $YN$  potential A [1].

#### 4. SUMMARY

An essential part of baryon-baryon interactions is the strong medium-range attraction, which in one-boson-exchange models is parameterized by exchange of a fictitious scalar-isoscalar meson with mass around 500 MeV. In extended meson exchange models this part is naturally generated by two-pion exchange contributions. As well as uncorrelated two-pion exchange, correlated contributions must be included in which the exchanged pions interact during their exchange; these terms in fact provide the main contribution to the intermediate-range interaction.



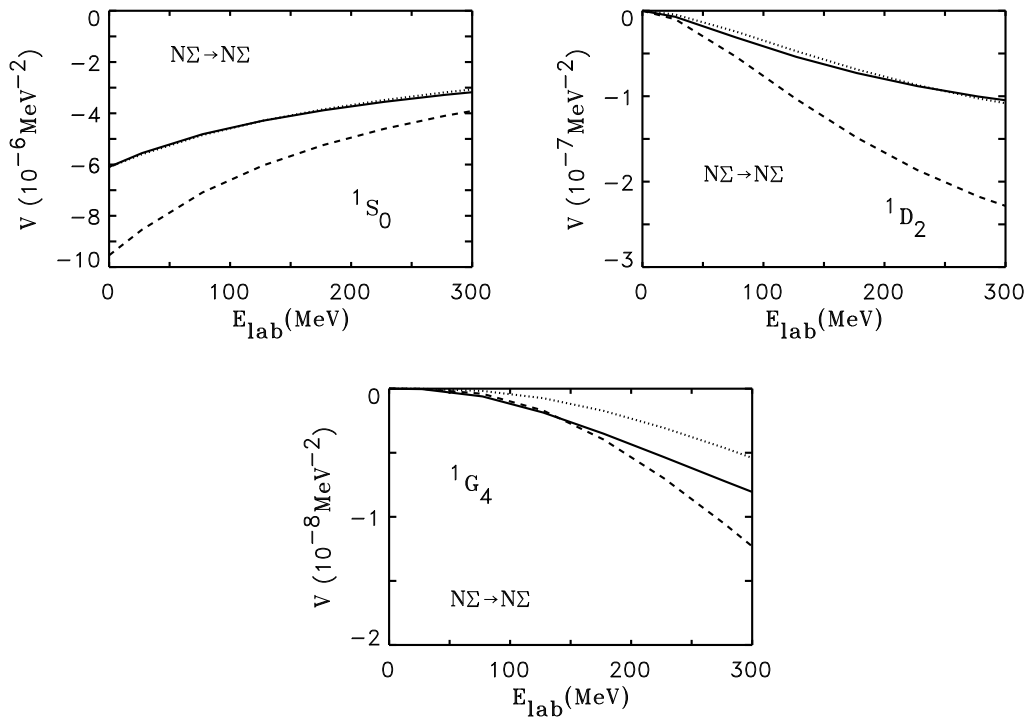


Figure 7. The  $\sigma$ -like part of the  $\Sigma N$  on-shell potential in various partial waves. Same description of curves as in Fig. 6.

In the scalar-isoscalar channel of the  $\pi\pi$  interaction the coupling to the  $K\bar{K}$  channel plays a strong role, which has to be explicitly included in any realistic model for energies near and above the  $K\bar{K}$  threshold. As kaon exchange is an essential part of hyperon-nucleon interactions a simultaneous investigation of correlated  $\pi\pi$  and  $K\bar{K}$  exchanges is clearly necessary. In Ref. [12] the correlated  $\pi\pi$  and  $K\bar{K}$  exchange contributions in various baryon-baryon channels have therefore been investigated within a microscopic model for the transition amplitudes of the baryon-antibaryon system ( $B\bar{B}'$ ) into  $\pi\pi$  and  $K\bar{K}$  for energies below the  $B\bar{B}'$  threshold. The correlations between the two mesons have been taken into account by means of  $\pi\pi - K\bar{K}$  amplitudes, determined in the field theoretic framework of Refs. [10, 11], which provide an excellent description of empirical  $\pi\pi$  data up to 1.3 GeV. With the help of unitarity and dispersion-theoretic methods, the baryon-baryon amplitudes for correlated  $\pi\pi$  and  $K\bar{K}$  exchange in the  $J^P = 0^+$  ( $\sigma$ ) and  $J^P = 1^-$  ( $\rho$ )  $t$ -channels have then been determined.

In the  $\sigma$  channel the strength of correlated  $\pi\pi$  and  $K\bar{K}$  exchange decreases with the strangeness of the baryon-baryon channels, becoming more negative. In the  $NN$  channel the scalar-isoscalar part of correlated exchanges is stronger by about a factor of 2 than in both hyperon-nucleon channels ( $\Lambda N$ ,  $\Sigma N$ ), and 3 to 4 times stronger than in the  $S = -2$  channels ( $\Lambda\Lambda$ ,  $\Sigma\Sigma$ ,  $N\Xi$ ).

With the current model it is now possible to reliably take into account correlated  $\pi\pi$  and  $K\bar{K}$  exchange in both the  $\sigma$  and  $\rho$  channels for various baryon-baryon reactions. This will be especially important in processes where only scant empirical data exist, as the elimination of the phenomenological  $\sigma$  and  $\rho$  exchanges considerably enhances the predictive power of baryon-baryon interaction models. Given the strong constraints on  $\sigma$  as well as  $\rho$  exchange from correlated  $\pi\pi$  exchange, a more sound microscopic model for the  $YN$  interaction can hence now be constructed, which can be used to address open

questions such as the role of SU(3) flavor symmetry, or the nature of the short range part of the  $BB'$  interaction arising from  $\omega$  exchange.

### Acknowledgements

We would like to thank the Special Research Centre for the Subatomic Structure of Matter at the University of Adelaide for support during the completion of this work. J.H. was supported by the DFG project no. 477 AUS-113/3/0.

### REFERENCES

1. B. Holzenkamp, K. Holinde and J. Speth, Nucl. Phys. A500 (1989) 485.
2. A. Reuber, K. Holinde and J. Speth, Nucl. Phys. A570 (1994) 543.
3. M.M. Nagels, T.A. Rijken and J.J. de Swart, Phys. Rev. D15 (1977) 2547.
4. M.M. Nagels, T.A. Rijken and J.J. de Swart, Phys. Rev. D20 (1979) 1633.
5. P.M.M. Maessen, T.A. Rijken and J.J. de Swart, Phys. Rev. C40 (1989) 2226.
6. U. Straub, et al., Nucl. Phys. A483 (1988) 686; Nucl. Phys. A508 (1990) 385c.
7. R. Machleidt, K. Holinde and Ch. Elster, Phys. Rep. 149 (1987) 1.
8. R.L. Jaffe, Phys. Rev. Lett. 38 (1977) 195; Phys. Rev. Lett. 38 (1977) 617(E).
9. H.-C. Kim, J.W. Durso and K. Holinde, Phys. Rev. C49 (1994) 2355.
10. D. Lohse, J.W. Durso, K. Holinde and J. Speth, Nucl. Phys. A516 (1990) 513.
11. G. Janssen, B.C. Pearce, K. Holinde, and J. Speth, Phys. Rev. D52 (1995) 2690.
12. A. Reuber, K. Holinde, H.-C. Kim and J. Speth, Nucl. Phys. A608 (1996) 243.
13. J. Haidenbauer, W. Melnitchouk and J. Speth, in preparation.
14. G. Höhler, F. Kaiser, R. Koch and E. Pietarinen, "Handbook of Pion-Nucleon Scattering" 4, Physics Data 12-1, Fachinformationszentrum, Karlsruhe, 1979.
15. K. Miyagawa and W. Glöckle, Phys. Rev. C48 (1993) 2576; K. Miyagawa, H. Kamada, W. Glöckle and V. Stoks, Phys. Rev. C51 (1995) 2905.